

# Features of proximal and distal excitatory synaptic inputs to layer V neurons of the rat medial entorhinal cortex

Virginia Medinilla, Orale Johnson and Sonia Gasparini

Neuroscience Center, Louisiana State University Health Sciences Center, New Orleans, LA 70112, USA

## Key points

- Layer V principal neurons of the entorhinal cortex receive the hippocampal output on their proximal and basal dendrites and send their axons to cortical areas, playing a fundamental role in memory processing.
- The apical dendrites of these neurons are rich in spines and extend to the entorhinal superficial layers, in the proximity of axons from cortical neurons, which could make synapses onto these spines.
- We stimulated afferent fibres in the superficial layers and recorded depolarizing responses in entorhinal layer V neurons, indicating that they receive excitatory inputs onto their distal dendrites.
- The responses were completely blocked by glutamatergic receptor antagonists; stimulation of distal afferents could initiate dendritic spikes, which propagated to the soma to generate an action potential.
- These results show that the distal dendrites of entorhinal layer V neurons have access to information that could affect the integration of the input from the hippocampus.

**Abstract** The entorhinal cortex (EC) has a fundamental function in transferring information between the hippocampus and the neocortex. EC layer V principal neurons are the main recipients of the hippocampal output and send processed information to the neocortex, likely playing an important role in memory processing and consolidation. Most of these neurons have apical dendrites that extend to the superficial layers and are rich in spines, which could be the targets of excitatory inputs from fibres innervating that region. We have used electrical stimulation of afferent fibres coupled with whole-cell patch-clamp somatic recordings to study the features of distal excitatory inputs and compare them with those of proximal ones. The amplitude of putative unitary excitatory responses was  $\sim 1.5$  times larger for distal compared with proximal inputs. The responses were purely glutamatergic, as they were abolished by a combination of AMPA and NMDA glutamatergic receptor antagonists. Blockade of  $I_h$  by 4-ethylphenylamino-1,2-dimethyl-6-methylaminopyrimidinium chloride (ZD7288) increased temporal summation; the increase was comparable for proximal and distal inputs. Proximal inputs initiated a somatic spike more reliably than distal ones; in some instances, somatic action potentials triggered by distal stimulation were preceded by dendritic spikes that fully propagated to the soma. Altogether, our results show that medial layer V entorhinal neurons receive excitatory synapses at distal dendritic locations, which gives them access to information encoded by inputs

V. Medinilla and O. Johnson contributed equally to this work.

to the superficial layers as well as the deep layers. These findings are fundamentally relevant to understanding the role of the EC in the formation and consolidation of episodic memory.

(Received 24 May 2012; accepted after revision 19 September 2012; first published online 24 September 2012)

**Corresponding author** S. Gasparini: Neuroscience Center, Louisiana State University Health Sciences Center, 2020 Gravier Street, New Orleans, LA 70112, USA. Email: sgaspa1@lsuhsc.edu

**Abbreviations** D,L-APV, D,L-2-amino-5-phosphonopentanoic acid; CNQX, 6-cyano-7-nitroquinoxaline-2,3-dione; DAMGO, Tyr-D-Ala-Gly-NMe-Phe-Gly-ol; EC, entorhinal cortex; PPF, paired-pulse facilitation; ZD7288, 4-ethylphenylamino-1,2-dimethyl-6-methylaminopyrimidinium chloride

## Introduction

The entorhinal cortex (EC) is a key structure within the medial temporal lobe memory system, having major afferent and efferent connections with the hippocampus. There is now considerable evidence that the EC is an essential component of the machinery used to encode declarative or episodic memory in the human brain (Witter & Wouterlood, 2002; Eichenbaum & Lipton, 2008), and that it is critically involved in neurological disorders. Entorhinal neurons appear to be severely and selectively affected in the early stages of Alzheimer's disease, and it has been suggested that such degeneration of the EC neuronal architecture would result in the memory and cognitive deficits associated with this pathology (Hyman *et al.* 1984; Braak & Braak, 1991). In addition, substantial evidence has accumulated that EC functions are impaired in temporal lobe epilepsy and schizophrenia (Scharfman, 2002; Schwarcz & Witter, 2002; Talbot & Arnold, 2002).

According to the traditional view, neurons in the entorhinal superficial layers (II–III) receive information from several cortical areas (Burwell & Amaral, 1998a), and relay it to the hippocampal formation via the perforant path (Steward & Scoville, 1976; Witter & Amaral, 1991). The hippocampus and subiculum, in turn, provide feedback pathways that end primarily in the deep layers (V and VI) of the EC (Swanson & Cowan, 1977; Sørensen & Shipley, 1979). Neurons in the deep layers give rise to long-range projections that go back to the neocortex (Swanson & Kohler, 1986; Insausti *et al.* 1997), thus closing a neocortical–hippocampal–neocortical loop. This notion, however, could be complicated by the observation that many entorhinal layer V neurons have prominent apical dendrites that extend and branch in tufts in the superficial layers (Hamam *et al.* 2000). These apical dendrites and tufts are rich in spines (Lingenhohl & Finch, 1991; Gasparini, 2011), and could therefore receive inputs from afferent fibres terminating on the superficial layer neurons. In the case of the medial EC, which processes mostly spatial information (Fyhn *et al.* 2004; Hargreaves *et al.* 2005), these fibres originate mainly from the postrhinal cortex (which in turn receives visual and visuo-spatial inputs; Naber *et al.* 1997; Burwell & Amaral, 1998a,b), the pre- and parasubiculum (Caballero-Bleda &

Witter, 1993), and the piriform cortex (Burwell & Amaral, 1998b). Other possible candidates for making excitatory synaptic contacts on the distal apical dendrites of EC layer V neurons include fibres from the amygdaloid complex, axons from layers II and III neurons, and recurrent collaterals from other layer V principal cells (Kohler, 1986; Canto *et al.* 2008).

Whereas the input from the hippocampus, which targets the deep layers and thus the basal dendrites and the proximal portion of the apical dendrites of entorhinal layer V neurons, has been characterized to some extent (Jones, 1987; Jones & Heinemann, 1988; Lingenhohl & Finch, 1991), inputs to the distal dendrites have only been described anatomically but not functionally (Wouterlood *et al.* 2004; Tolner *et al.* 2005).

We have used somatic whole-cell patch-clamp recordings coupled to electrical stimulation of afferent fibres to show that the distal dendrites of EC layer V principal neurons receive functional excitatory glutamatergic synaptic inputs, and to compare the properties of these inputs with those made onto the proximal dendrites. Proximal and distal synapses differ in the amplitude of the unitary synaptic response (which is larger for distal synapses) and the ability to elicit a somatic action potential output. Taken together, our results suggest that entorhinal layer V neurons could have more complicated functions than just being a relay between the hippocampus and the neocortex, and shed new light on the function of these neurons in the formation and consolidation of episodic memory.

## Methods

### Slice preparation and maintenance

EC slices (400  $\mu\text{m}$  thick) were prepared from 7- to 9-week-old male Sprague–Dawley rats, according to methods approved by the Louisiana State University Health Sciences Center Institutional Animal Care and Use Committee. Rats were deeply anaesthetized with an intraperitoneal injection of ketamine and xylazine (90 and 10  $\text{mg kg}^{-1}$ , respectively; additional doses were administered if the toe-pinch reflex persisted), perfused through the ascending aorta with an oxygenated ice-cold

solution, and decapitated. Brains were removed and slices were cut using a vibratome, kept in a holding chamber at 36°C for 1 h, and at room temperature for the rest of the day (<6 h). Individual slices were transferred to a submerged recording chamber, where EC layer V principal cells were visualized using a Zeiss Axioskop fit with differential interference contrast (DIC) optics under infrared illumination. Only cells that showed a prominent apical dendrite emerging from the soma were selected for recording.

### Electrophysiological recordings

The external solution used for recordings contained (in mM): NaCl, 125; KCl, 2.5; NaHCO<sub>3</sub>, 25; NaH<sub>2</sub>PO<sub>4</sub>, 1.25; CaCl<sub>2</sub>, 2; MgCl<sub>2</sub>, 1; dextrose, 25; and was saturated with 95% O<sub>2</sub> and 5% CO<sub>2</sub> at 34–36°C (pH 7.4). Whole-cell patch-clamp somatic recordings were performed in current-clamp configuration using a Dagan BVC-700 amplifier in the active 'bridge' mode. Patch pipettes had a resistance of 2–4 MΩ when filled with a solution containing (in mM): potassium-methylsulphonate, 125; Hepes, 10; NaCl, 4; Mg<sub>2</sub>ATP, 4; Tris<sub>2</sub>GTP, 0.3; phosphocreatine, 14 (pH 7.3). Series resistances were constantly monitored, and were usually in the order of 10–25 MΩ.

Electrical stimulation was achieved by delivering constant current pulses to presynaptic afferent fibres through a tungsten bipolar electrode placed in the proximal dendritic region of EC layer V cells to stimulate fibres from the subiculum (40–100 μm from the soma), or in the EC superficial layers (>400 μm from the soma) to stimulate fibres making synapse onto the distal portion of the apical dendrite (Fig. 1). In some experiments, the distal stimulating electrode was placed in the vicinity of the apical dendrite, at ~400 μm from the soma, yielding results similar to the stimulation of the superficial layers. In a set of experiments proximal and distal stimulation were conducted simultaneously, and the postsynaptic responses were recorded from the same cell.

In our initial studies, the excitatory component of the postsynaptic responses was isolated by perfusing GABA<sub>A</sub> antagonists (gabazine, 12.5–25 μM; bicuculline, 5–20 μM; or picrotoxin 100 μM). Because the perfusion of GABA<sub>A</sub> antagonists induced hyperexcitability in the slices (Fig. 2), we used the μ-opioid agonist peptide Tyr-D-Ala-Gly-NMe-Phe-Gly-ol (DAMGO; 2.5 μM; Sigma-Aldrich, St. Louis, MO, USA) to isolate the excitatory component of the responses in subsequent experiments.

Minimal stimulation of putative single fibres was achieved by decreasing the intensity of stimulation until non-detectable postsynaptic responses (i.e. failures) were obtained in at least 50% of the trials (Raastad *et al.* 1992). The ability to evoke a response at a given stimulus level

was very sensitive to exact electrode placement, such that a 5–10 μm movement of the stimulating electrode produced a drastic change in the responses. In addition, in most cases there was a clear gap between the apparent failures and the smallest detectable responses (Fig. 3). The rise time constants were calculated by averaging all the episodes that produced a response, and fitting the region between 10% and 90% of the response amplitude with an exponential function. Paired-pulse facilitation (PPF) was evoked with paired stimuli (50 ms interval), and expressed as the ratio of the amplitude of the second EPSP to that of the first for the average of all traces (failures + responses). For this calculation, only experiments that yielded responses on the first stimulus for more than one-fifth of the trials were considered, to avoid dividing by a very small number, which would provide an inaccurately high PPF value.

Membrane input resistance was calculated by fitting the current–voltage plots of the membrane potential deflections produced by 500 ms current injections, measured at steady state (i.e. at the end of the step).

AMPA- and NMDA-mediated components were blocked by the use of external 6-cyano-7-nitroquinoline-2,3-dione (CNQX; 25 μM; Tocris Bioscience, Minneapolis, MN, USA) and D,L-2-amino-5-phosphonopentanoic acid (D,L-APV; 50 μM), respectively. D,L-APV was obtained from the National Institute of Mental Health's Chemical Synthesis and Drug Supply Program. Blockade of I<sub>h</sub> was achieved by administration of 4-ethylphenylamino-1,2-dimethyl-6-methylaminopyrimidinium chloride (ZD7288; 20 μM; Tocris Bioscience); in these experiments, D,L-APV (50 μM) was also added to the solutions to remove the NMDA component of the responses. Trains (20 Hz) of five action potentials were delivered to determine the level of temporal summation; as ZD7288 in some instances induced an increase in the amplitude of the first EPSP, the intensity of stimulation was decreased to match the amplitude recorded in control conditions.

The NEURON simulation program (Hines & Carnevale, 1997) was used to simulate a multicompartmental model of an entorhinal layer V neuron with proximal and distal synapses impinging upon the apical dendrite at 100 and 400 μm from the soma, respectively. The somatic compartment was a cylinder 10 μm in diameter and 10 μm in length. The dendrite was 2 μm in diameter nearest the soma, tapering gradually to 0.5 μm at 400 μm, and remaining at a constant diameter to the termination of the dendrite at 700 μm. Passive properties were a membrane resistance of 10 kΩ cm<sup>2</sup>, an axial resistance of 150 Ω cm<sup>-1</sup> and a capacitance of 1 μF cm<sup>-2</sup>. The synaptic conductances were modelled using a biexponential function with rise and decay time constants of 0.1 and 2 ms for AMPA, and 1 and 20 ms for NMDA components, respectively, and a reversal potential of 0 mV (Gasparini *et al.* 2004). The Mg<sup>2+</sup> block of the

NMDA receptors was as in Jahr & Stevens (1990), with  $[Mg^{2+}]_o = 1$  mM.

Data are reported as means  $\pm$  SEM. Statistical comparisons were performed using the Mann–Whitney U test (between proximal and distal groups) and the Wilcoxon matched-pairs signed-ranks test (to analyse effects within a group). Means were considered to be significantly different when  $P < 0.05$ .

## Results

The distal portion of the apical dendrites of entorhinal layer V neurons has a high density of spines (Gasparini, 2011), and within this region the spines are in close proximity to axons from various cortical areas and the pre-subiculum (Wouterlood *et al.* 2004). The spatial proximity of the apical spines and cortical axonal terminals led us to hypothesize the existence of functional excitatory inputs to the distal dendrites from these cortical areas. In the present work, we set out to characterize these distal inputs and compare their features with those of the proximal inputs conveying information from the hippocampus and subiculum.

### Isolation of the excitatory response

In order to isolate the excitatory component of the synaptic responses of EC layer V cells, GABA<sub>A</sub> antagonists were

added to the external solution used for the recordings. All GABA<sub>A</sub> antagonists tested (gabazine, 12.5–25  $\mu$ M; bicuculline, 5–20  $\mu$ M; or picrotoxin, 100  $\mu$ M) induced hyperexcitability, which was observed in 37% and 100% of the cells studied upon proximal and distal stimulation, respectively (Fig. 2A and B). We define hyperexcitability as bursts of action potentials initiating during or just after the synaptic response, and outlasting the original stimulus by hundreds of milliseconds, presumably due to activation of recurrent excitation that was no longer effectively suppressed by inhibitory interneurons due to the GABA<sub>A</sub> receptor blockade. For this reason, we had to identify a different pharmacological approach to isolate the excitatory responses.

DAMGO, a  $\mu$ -opioid agonist peptide, has been shown to greatly reduce inhibitory transmission in the hippocampus by hyperpolarizing inhibitory interneurons and decreasing neurotransmitter release (Capogna *et al.* 1993; Svoboda & Lupica, 1998), and to allow the isolation of excitatory postsynaptic currents in CA3 hippocampal pyramidal neurons in organotypic slices, which show a high degree of recurrent excitation (Hanson *et al.* 2006). We therefore tested the effect of DAMGO (2.5  $\mu$ M) on synaptic transmission in the medial EC. DAMGO did not induce the hyperexcitability that was seen with the use of GABA<sub>A</sub> blockers, but strongly attenuated the postsynaptic inhibitory response resulting from stimulation at both

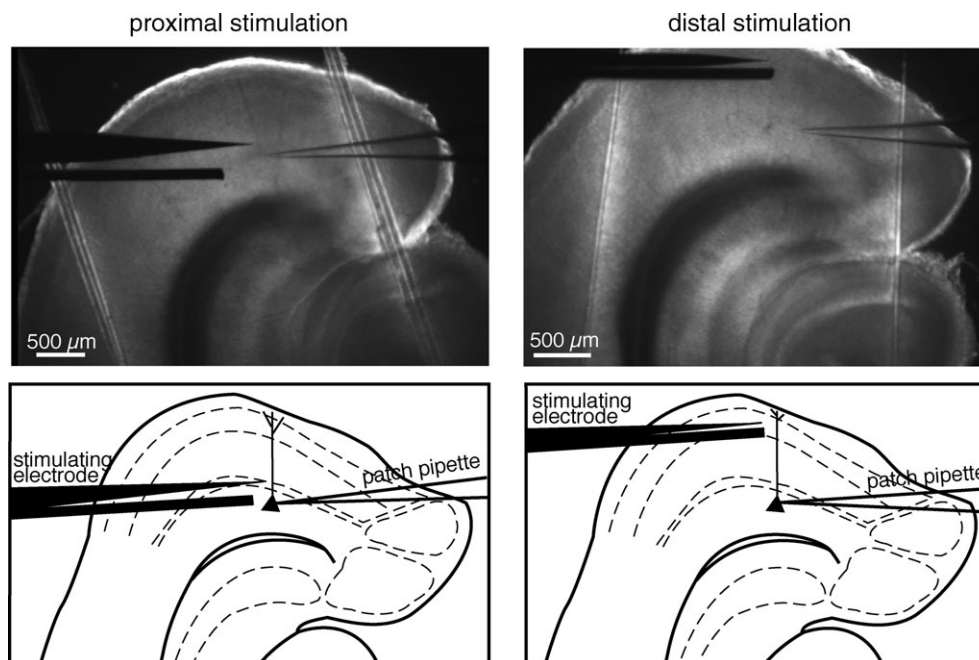


**Figure 1. Recording configurations**

Low-magnification images and schematic diagrams of EC slices showing the experimental configuration of proximal vs. distal electrical stimulation. The bipolar stimulating electrode was placed at  $\sim 100$   $\mu$ m from the soma to stimulate proximal afferent fibres, or in the EC superficial layers ( $> 400$   $\mu$ m from the soma) to stimulate distal ones. These pictures also enabled us to confirm that the neuron we were recording from was in the medial portion of entorhinal layer V.

proximal and distal synapses, such that the monosynaptic excitatory response could be studied in isolation (Fig. 2C and D). On the other hand, DAMGO did not affect the excitability of entorhinal layer V neurons, evaluated as changes in the parameters of action potentials elicited by the injection of a 2 ms depolarizing current step. The threshold was  $-57.4 \pm 2.0$  mV under control conditions vs.  $-58.5 \pm 2.1$  mV in the presence of DAMGO  $2.5 \mu\text{M}$  ( $n = 11$ ;  $P > 0.5$ ); the half-width was  $1.1 \pm 0.1$  ms vs.  $1.2 \pm 0.1$  ms ( $n = 11$ ;  $P > 0.05$ ). DAMGO was therefore used in the subsequent experiments.

### Putative unitary excitatory synaptic responses

Minimal stimulation of afferent fibres was used to characterize putative unitary excitatory responses. All the conditions reported by Raastad *et al.* (1992) for the stimulation of a single presynaptic fibre were met (see Methods).

The latencies to the onset of the EPSP were 2–4 ms for stimulation of both proximal and distal inputs (measured from the beginning of the stimulus artefact), arguing in favour of monosynaptic connections between the afferent fibres and the postsynaptic EC layer V neurons (Sayer *et al.* 1990). The average unitary excitatory response was  $\sim 1.5$  times larger for distal than for proximal synapses

when recorded at the soma ( $0.45 \pm 0.03$  mV,  $n = 25$  for distal vs.  $0.29 \pm 0.03$  mV,  $n = 20$  for proximal,  $P < 0.01$ ; Fig. 3A–D), as can be also appreciated in the plot of the cumulative frequency distribution (Fig. 3E). This result is counterintuitive given the cable properties of the dendrites, which should attenuate to a greater extent the amplitude of synaptic inputs located at distances further away from the soma (Rall, 1967). On the other hand, the rise time constants of the EPSPs were significantly slower for distal inputs than for proximal ( $4.3 \pm 0.3$  ms vs.  $2.4 \pm 0.2$  ms, respectively,  $P < 0.0001$ ; Fig. 3F), providing evidence that the stimulation of EC superficial layers activated distal synapses, as the kinetics of the distal inputs would be subject to more dendritic filtering than those of proximal ones (Rall, 1967). PPF was comparable for proximal and distal inputs ( $2.6 \pm 0.5$  mV,  $n = 16$  vs.  $2.8 \pm 0.3$  mV,  $n = 22$ , respectively,  $P > 0.3$ ; Fig. 3G).

We used a multicompartmental model of an entorhinal layer V neuron, consisting of a tapered dendrite attached to a soma implemented in NEURON to simulate the somatic EPSP resulting from activation of proximal ( $100 \mu\text{m}$ ) and distal synapses ( $400 \mu\text{m}$ ). We found that, in order to replicate the experimental results with respect to the difference in EPSP amplitude observed at the soma, the AMPA conductance for the distal synapse had to be

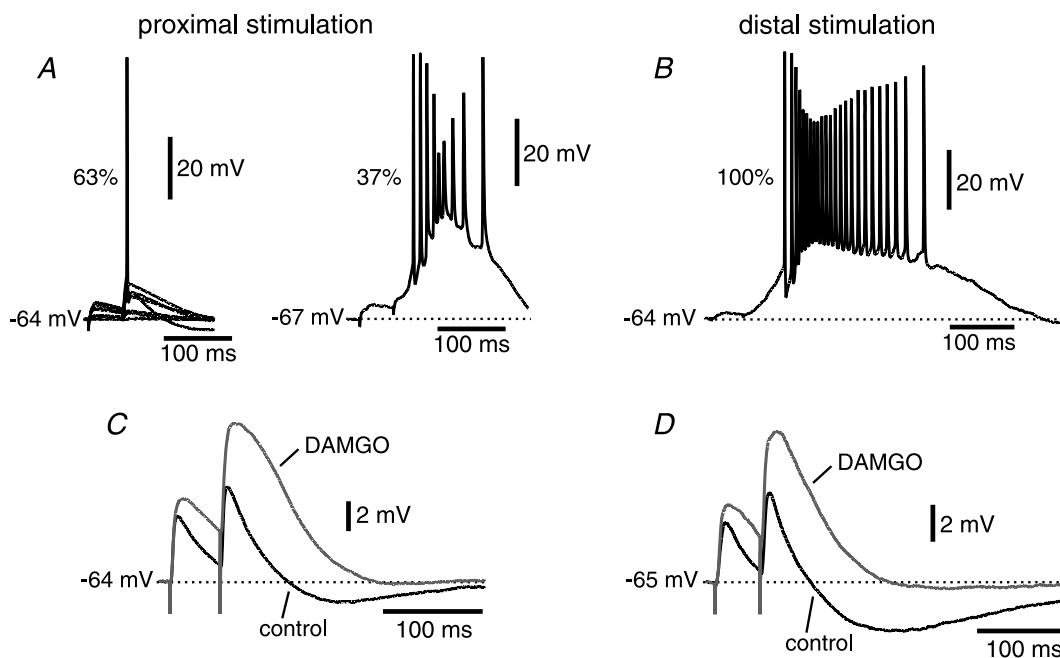


**Figure 2. Tyr-D-Ala-Gly-NMe-Phe-Gly-ol (DAMGO) removes inhibition without inducing the stimulation-induced hyperexcitability observed in the presence of GABA<sub>A</sub> receptor antagonists**

A, electrical stimulation of proximal afferents in the presence of GABA<sub>A</sub> antagonists induced hyperexcitability in  $\sim 1/3$  (16 out of 43) of the cells studied. B, stimulation of distal afferents under the same conditions led to hyperexcitability in all of the cells studied (20 out of 20). C and D, the  $\mu$ -opioid agonist peptide DAMGO effectively removed inhibition but did not induce hyperexcitability upon stimulation of either proximal or distal afferents, respectively.

approximately three times as large as the proximal one. In addition, we found that the contribution of the NMDA conductance was negligible due to the relatively small amplitude of the local depolarizations (a maximum of 2.5 mV at the distal location).

### Effects of glutamatergic receptor antagonists

AMPA and NMDA glutamatergic receptor antagonists were used to study the nature of the neurotransmitters contributing to the excitatory component of the synaptic responses.

Bath application of the AMPA–kainate antagonist CNQX (25  $\mu\text{M}$ ) almost completely abolished the responses originated by electrical stimulation of both proximal and distal afferent fibres ( $92 \pm 1\%$ ,  $n = 17$  vs.  $97 \pm 1\%$ ,  $n = 15$ , respectively,  $P < 0.01$ ; Fig. 4). Subsequent addition of the NMDA receptor antagonist D,L-APV (50  $\mu\text{M}$ ) completely abolished the remaining excitatory component of the response for both proximal and distal inputs (Fig. 4A and D), demonstrating that transmission is

purely glutamatergic at both sets of synapses. On the other hand, perfusion of D,L-APV (50  $\mu\text{M}$ ) alone significantly decreased the amplitude of the EPSPs proximally ( $4.9 \pm 0.3$  mV in control vs.  $3.8 \pm 0.4$  mV with D,L-APV,  $n = 12$ ,  $P < 0.003$ ; Fig. 5B) and distally ( $4.3 \pm 0.3$  mV in control vs.  $3.6 \pm 0.4$  mV with D,L-APV,  $n = 11$ ,  $P < 0.02$ ; Fig. 5F). In addition, as expected, the blockade of NMDA glutamatergic receptors had a significant effect on the kinetics of both proximal and distal synaptic responses, decreasing the decay time constant (from  $62 \pm 3$  ms to  $42 \pm 4$  ms for proximal,  $n = 12$ ,  $P < 0.003$ ; and from  $54 \pm 5$  ms to  $36 \pm 4$  ms for distal stimulation,  $n = 11$ ,  $P < 0.01$ ; Fig. 5C and G, respectively) and the integral of the response (the area under the curve, or AUC, from  $0.60 \pm 0.06$  mV·ms to  $0.37 \pm 0.06$  mV·ms for proximal,  $n = 12$ ,  $P = 0.0005$ ; and from  $0.57 \pm 0.07$  mV·ms to  $0.34 \pm 0.04$  mV·ms for distal,  $n = 11$ ,  $P < 0.01$ ; Fig. 5D and H, respectively). The amplitude, the decay time constant and the integral of the EPSPs in control conditions were not significantly different for proximal and distal synapses ( $P > 0.09$ ,  $P > 0.1$  and  $P > 0.5$ , respectively).

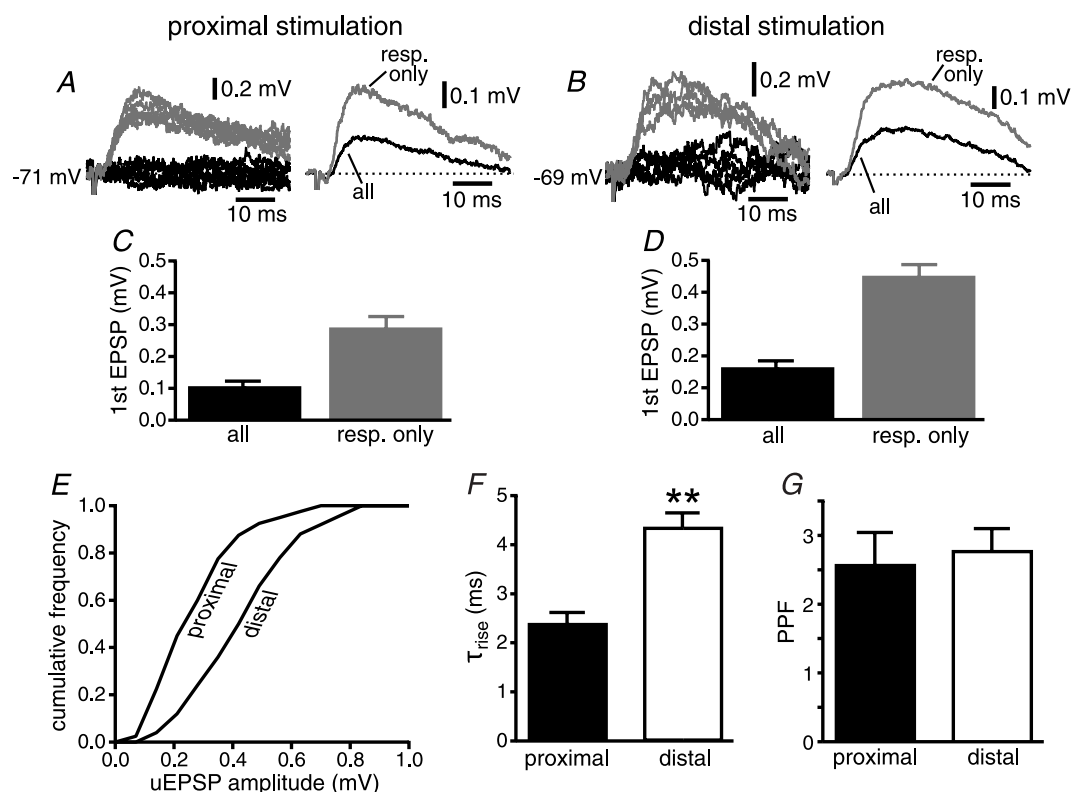


**Figure 3. Minimal stimulation of afferent fibres and putative unitary responses**

A, proximal stimulation. On the left, representative traces corresponding to responses (grey traces) and failures of transmission (black) are shown for a single cell. On the right, the average of the responses (resp. only, grey trace) is superimposed to the average of all episodes (all, black). B, same for distal stimulation. C and D, group data for proximal and distal stimulation, respectively. E, normalized cumulative frequency distribution of average amplitude of the putative unitary EPSPs (uEPSP) for proximal and distal stimulation. F, group data for the value of the rise time constant ( $\tau_{\text{rise}}$ ) for proximal and distal EPSPs (\*\* $P < 0.01$ ). G, group data of paired-pulse facilitation (PPF) for responses to proximal and distal stimulation.

### Role of $I_h$ in temporal summation

A differential distribution of  $I_h$  along the apical dendrites of CA1 neurons and layer V neocortical pyramidal neurons has been shown to deeply affect temporal summation at distal dendritic locations (Magee, 1999; Williams & Stuart, 2000). We therefore used the selective  $I_h$  blocker ZD7288 ( $20 \mu\text{M}$ ; Gasparini & DiFrancesco, 1997; Magee, 1999) to determine the role of h-channels in neuronal excitability, and temporal summation for proximal and distal inputs in EC layer V neurons. Bath application of ZD7288 induced a hyperpolarization of the membrane potential of  $3.6 \pm 0.9 \text{ mV}$  ( $n = 11$ ), which was compensated by the injection of depolarizing current, to remove the effect of a change in driving force on EPSP amplitude. In addition, ZD7288 induced a 28% increase of the input resistance at steady state, measured from 500 ms steps (see Methods; from  $156 \pm 12 \text{ M}\Omega$  to  $200 \pm 12 \text{ M}\Omega$ ,  $n = 13$ ,  $P < 0.002$ ; Fig. 6A–C). This change is considerably smaller than the 136% increase observed in CA1 neurons following the perfusion of ZD7288 (from  $65 \pm 5 \text{ M}\Omega$  to  $149 \pm 10 \text{ M}\Omega$ ,

$n = 11$ ; see Supplemental Material); the relatively weaker effect of ZD7288 and the overall higher input resistance for entorhinal layer V neurons support the conclusion that  $I_h$  is expressed at a lower level in these neurons than in CA1 pyramidal neurons.

In the set of experiments designed to study temporal summation, the synaptic response was mostly recorded from the same postsynaptic neuron, while proximal and distal inputs were alternatively stimulated every 30 s. The rise time constants were significantly slower for distal inputs than for proximal ( $4.7 \pm 0.2 \text{ ms}$ ,  $n = 11$  vs.  $2.2 \pm 0.2 \text{ ms}$ ,  $n = 11$ , respectively,  $P < 0.0001$ ; Fig. 6D), again providing evidence of activation of synapses localized further away from the soma than proximal ones. It is worth noting that ZD7288 did not significantly affect PPF for the first two EPSPs for both proximal and distal inputs (from  $2.0 \pm 0.2$  to  $2.1 \pm 0.1$ ,  $n = 9$ ,  $P > 0.2$ ; and from  $2.0 \pm 0.1$  to  $2.4 \pm 0.2$ ,  $n = 12$ , respectively,  $P > 0.05$ ), arguing in favour of a postsynaptic effect of the drug. ZD7288 significantly increased temporal summation, measured as the ratio of the amplitude of the fifth EPSP to

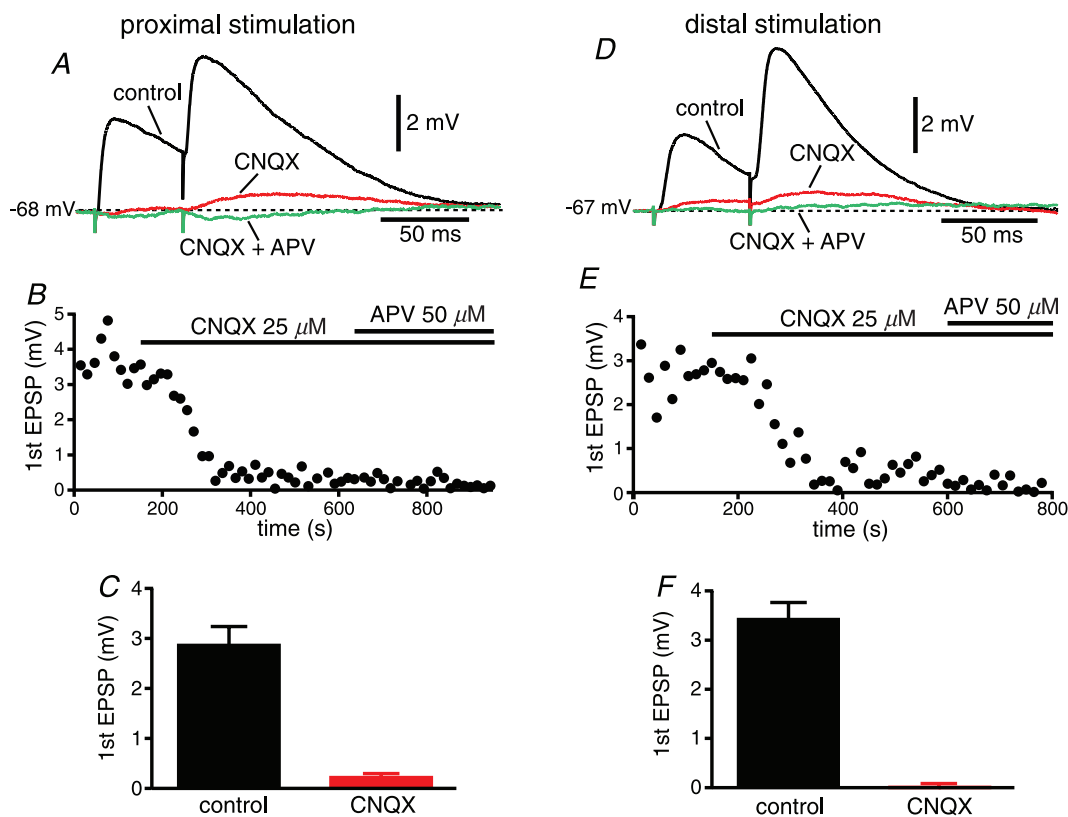


**Figure 4. Perfusion of both AMPA and NMDA receptor antagonists completely eliminates the excitatory component of the synaptic response**

A, EPSPs recorded in control conditions (black), in the presence of the AMPA receptor antagonist 6-cyano-7-nitroquinoxaline-2,3-dione (CNQX;  $25 \mu\text{M}$ , red), and in the presence of both CNQX and the NMDA receptor antagonist  $D,L$ -2-amino-5-phosphonopentanoic acid ( $D,L$ -APV;  $50 \mu\text{M}$ , green), in response to stimulation of proximal afferents. B, time course of the amplitude of the first EPSP in the presence of CNQX, and with further addition of  $D,L$ -APV. C, group data of the amplitude of the first EPSP under control conditions and in the presence of CNQX. D–F, same for stimulation of distal afferents.

that of the first for 20 Hz trains, proximally ( $2.5 \pm 0.4$  in control *vs.*  $3.0 \pm 0.4$  with ZD7288, a 26% increase,  $n = 9$ ,  $P < 0.05$ ; Fig. 6E and G) and distally ( $2.3 \pm 0.2$  in control *vs.*  $3.0 \pm 0.3$  with ZD7288, a 31% increase,  $n = 12$ ,  $P < 0.005$ ; Fig. 6F and H). These results are in contrast with what has been reported in hippocampal CA1 neurons, where the effect of ZD7288 is highly location dependent (Magee, 1999). To support our findings, we replicated similar experiments in hippocampal CA1 neurons, and observed an  $18 \pm 5\%$  increase of temporal summation for proximal inputs and an  $85 \pm 17\%$  increase for distal ones in the presence of ZD7288 ( $n = 8$ ; see Supplemental Material), as expected from a higher  $I_h$  expression at distal sites (Magee, 1999). To further exclude the possibility that differences in the effect of ZD7288 on temporal summation between proximal and distal synapses would become apparent in entorhinal layer V neurons with longer trains, we extended our observation to 20 Hz trains of 10 stimuli. ZD7288 induced a  $43 \pm 10\%$  ( $n = 11$ ) increase of temporal summation (measured as the ratio of the amplitude of the 10th EPSP to that of the first) for proximal synapses and a  $52 \pm 18\%$

increase for distal synapses ( $n = 13$ ), showing that also in this case the blockade of  $I_h$  had a comparable effect at proximal and distal locations. In the case of CA1 pyramidal neurons, ZD7288 induced a  $45 \pm 10\%$  increase of temporal summation (measured as the ratio of the amplitude of the 10th EPSP to that of the first) proximally and a  $120 \pm 23\%$  increase distally ( $n = 7$ ), confirming the highly location-dependent effect of  $I_h$  blockade in these neurons. Taken together, these data argue against a gradient of  $I_h$  expression from the soma to the distal apical dendrite in entorhinal layer V neurons.

### Generation of a somatic output

Finally, we tested whether the activation of proximal or distal inputs was able to elicit a somatic action potential. We therefore gradually increased the intensity of stimulation to recruit a progressively larger number of afferent fibres and generate increasingly larger EPSPs, which could eventually reach the threshold for an action potential (Fig. 7). When proximal inputs were stimulated, a somatic action potential was generated in all of the EC

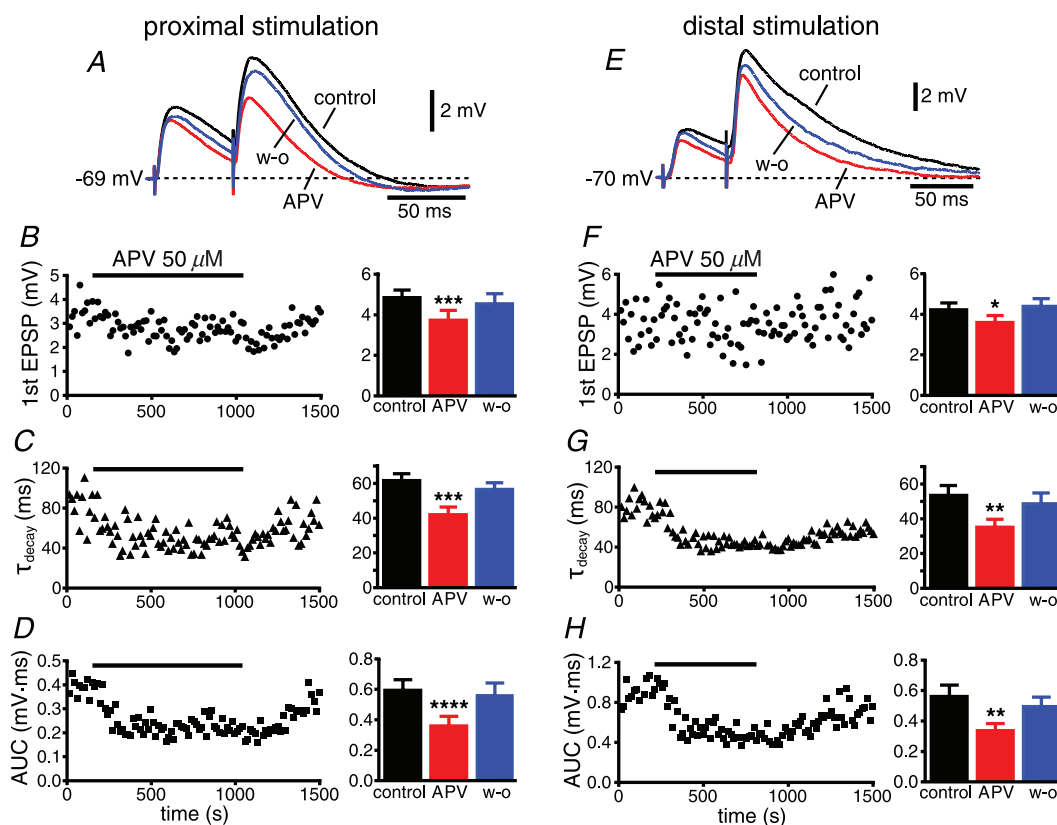


**Figure 5. NMDA receptor antagonists significantly reduce the EPSP**

A, EPSPs recorded in control conditions (black), during the perfusion of the glutamatergic NMDA receptor antagonist D,L-2-amino-5-phosphonopentanoic acid (D,L-APV; red), and upon wash-out (blue). The time courses of the amplitude of the first EPSP, the decay time constant ( $\tau_{\text{decay}}$ ) and the area under the curve (AUC) are shown in B–D, respectively, with the group data on the right. E–H, an example of stimulation of distal afferents, with the group data also shown on the right. \* $P < 0.02$ ; \*\* $P < 0.01$ ; \*\*\* $P < 0.003$ ; \*\*\*\* $P = 0.0005$ .

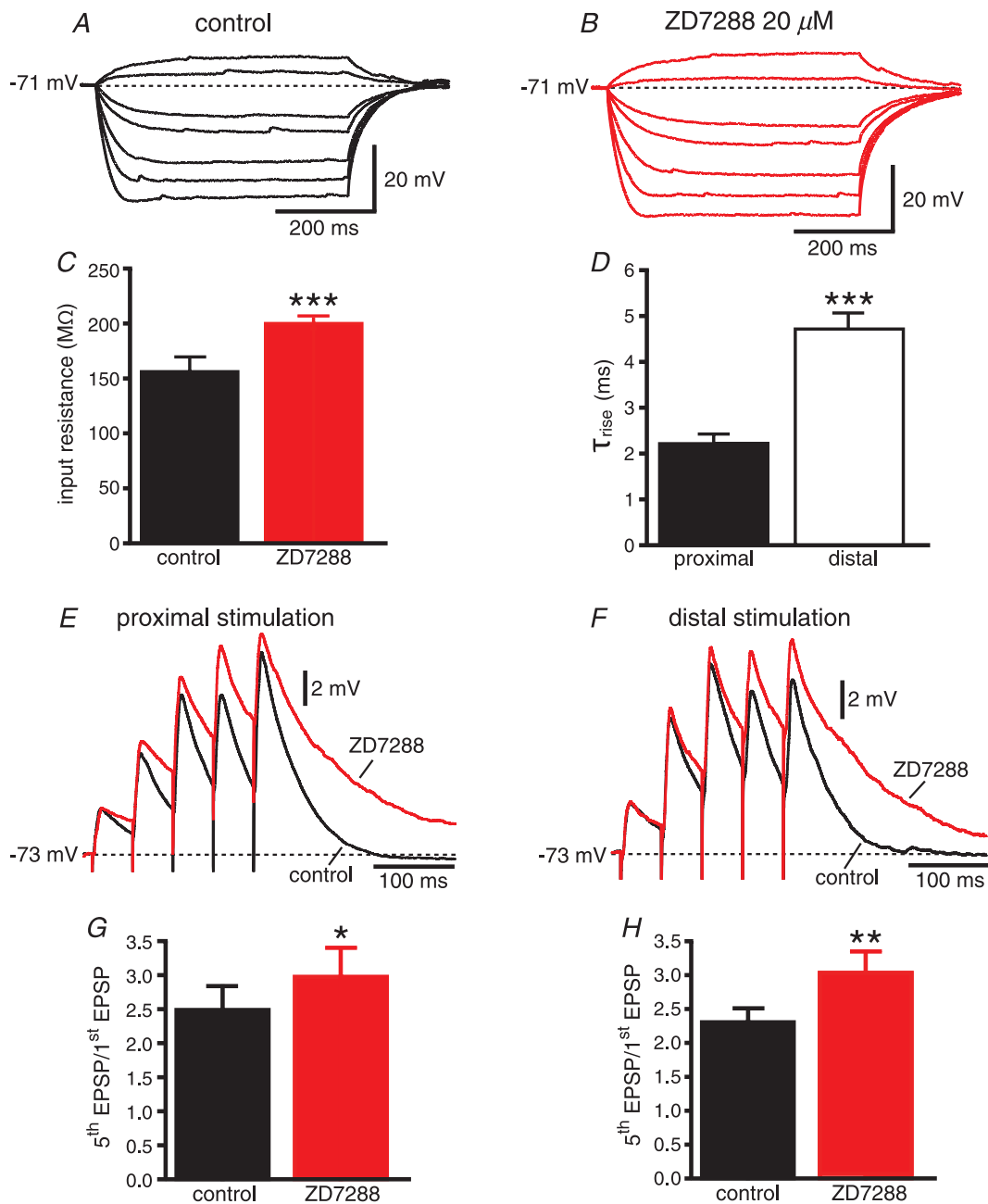


**Figure 6. Blockade of h-channels increases summation of excitatory responses in a location-independent manner in entorhinal layer V neurons**

A, membrane potential recordings in response to 500 ms current injections ranging from  $-200$  pA to  $50$  pA recorded under control conditions and in the presence of 4-ethylphenylamino-1,2-dimethyl-6-methylaminopyrimidinium chloride (ZD7288;  $20 \mu\text{M}$ ; B). C, plot of the average steady state input resistance (see Methods) in control conditions and in the presence of ZD7288. D, average data of the rise time constants for proximal and distal responses. E, EPSPs recorded under control conditions (black), and in the presence of ZD7288 (red), in response to a 20 Hz train of 5 electrical stimuli of proximal afferents. F, same for stimulation of distal inputs. G and H, average data show that summation (expressed as the ratio of the amplitude of the fifth EPSP to that of the first) increases by  $\sim 26\%$  and  $\sim 31\%$  in the presence of ZD7288 in comparison to control conditions for proximal and distal inputs, respectively. Proximal and distal recordings were performed in the same cell.  $*P < 0.05$ ,  $**P < 0.005$  and  $***P < 0.0005$ .

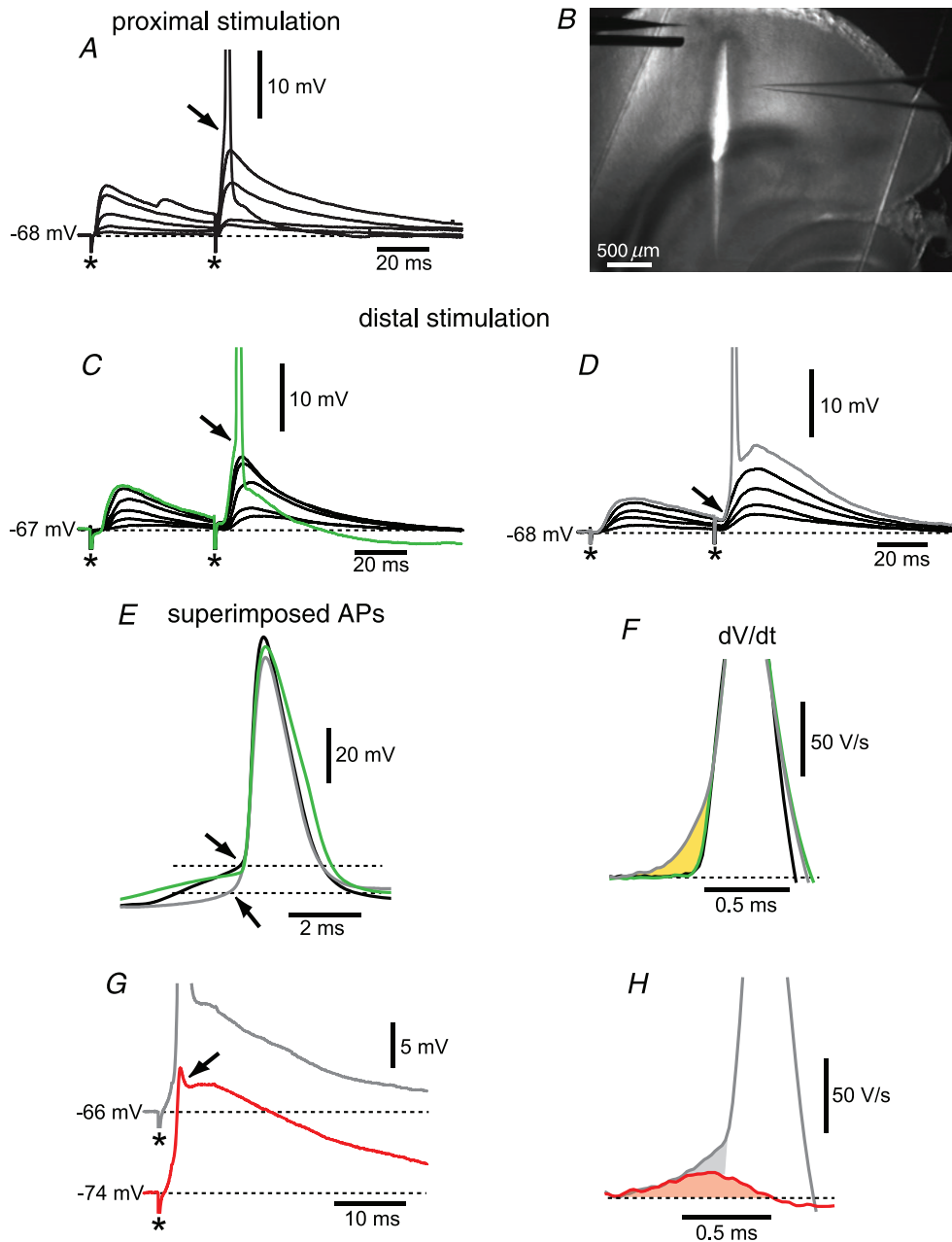


**Figure 7. Electrical stimulation of increasing intensities can evoke all-or-none somatic action potentials**

*A*, proximal stimulation can always evoke all-or-none somatic action potentials after removal of inhibition (action potentials are truncated at  $-40$  mV). *B*, low-magnification image showing the cut made to sever proximal afferent fibres that could be activated by distal stimulation. *C*, action potentials characterized by a relatively high voltage threshold (see arrow and green trace) were recorded in 18 out of 41 neurons during distal stimulation using the configuration shown in *B*. *D*, seven neurons were characterized by an apparent lower threshold (see arrow and grey trace). *E*, the traces for the supra-threshold responses in *A*, *C* and *D* are superimposed to show the difference in apparent voltage threshold for the action potential (arrows). *F*, superimposition of the  $dV/dt$  of the traces shown in *E* to show the slow ramp component characteristic of a dendritic spike that fully propagates to the soma (grey trace) in comparison to the steep rising phase of an action potential originated in the soma/axon region. *G*, hyperpolarization of the membrane potential via DC current injection prevents the initiation of a somatic action potential, and as a result only a spikelet is recorded in the somatic voltage trace (see red trace and arrow). *H*, the  $dV/dt$  component of the spikelet (red trace and shaded area) precedes and underlies the slow ramp component present when a dendritic spike fully propagates to the soma generating an action potential (grey trace and shaded area). \* denotes the stimulus artefact.

layer V neurons tested (19 out of 19). In these recordings, the supra-threshold responses were characterized by the steep rising phase of the action potential occurring on top of the slower EPSP (the transition is indicated by the arrow in Fig. 7A). This type of response is characteristic of spikes that are initiated when the EPSP-mediated depolarization reaches the threshold in the soma/axon region (Anderson *et al.* 1987; Gasparini *et al.* 2004). As for the stimulation of distal fibres, in order to eliminate the possibility that the higher intensities of stimulation could activate axons that made contact proximally on the dendritic tree, we severed the proximal fibres by making a small knife cut parallel to the apical dendrites of layer V cells (Fig. 7B). With this configuration, electrical stimulation of distal afferents originated a postsynaptic spike in 25 out of 41 neurons. Of the neurons that originated an output spike, most showed a supra-threshold response similar to that generated by proximal stimulation, i.e. characterized by a clear transition between the synaptic response and the action potential (see arrow in Fig. 7C; the average threshold was  $-54.1 \pm 0.9$ ,  $n = 18$ ). Seven of the 25 neurons, however, were characterized by an apparent lower voltage threshold ( $-64.0 \pm 1.0$ ,  $n = 7$ ; see arrow in Fig. 7D); the difference in the apparent spike voltage threshold can be better appreciated in Fig. 7E, where the action potentials recorded in these different situations are superimposed. An apparent lower threshold for somatic action potentials has been reported in CA1 pyramidal neurons, when a spike was initiated in the dendrites and fully propagated to the soma, as shown by simultaneous dendritic and somatic recordings (Gasparini *et al.* 2004). To investigate if this was the case also in entorhinal layer V neurons, we compared the first derivative ( $dV dt^{-1}$ ) of the voltage traces for the supra-linear responses shown in Fig. 7E. In this case, the  $dV dt^{-1}$  of the action potentials characterized by a higher voltage threshold (black and green traces) show a relatively flat baseline with a single steep, large (maximal amplitude  $\sim 300$  V s $^{-1}$ ) component, which is reportedly caused by the invasion of the soma by an axonal action potential (Fig. 7F; Colbert & Johnston, 1996; Gasparini *et al.* 2004). On the other hand, for lower threshold spikes like the one in Fig. 7D (grey trace), the same large component in the  $dV dt^{-1}$  profile was preceded by a shallower component (see shaded area in yellow). In CA1 neurons, this 'ramp' component was observed only when a dendritic spike reliably propagated to the soma to initiate a somatic action potential (Gasparini *et al.* 2004), and therefore led us to hypothesize that the somatic spike in Fig. 7D resulted from a dendritic spike. In support of this finding, we sought to uncouple the initiation of the dendritic spike from the generation of the somatic action potential. To this end, we stimulated distal afferents and, after eliciting somatic action potentials with an apparent lower threshold like the one in Fig. 7D, we hyperpolarized the membrane potential by injecting

DC current in order to weaken the forward propagation of dendritic spikes, as shown in CA1 pyramidal neurons (Gasparini *et al.* 2004; Makara *et al.* 2009). Figure 7G shows that at hyperpolarized membrane potentials (more negative than  $-71$  mV) only a spikelet could be recorded in the somatic voltage trace, indicative of a spike that was initiated in the dendrite but did not fully propagate to the soma (Golding *et al.* 2002; Gasparini *et al.* 2004). By uncoupling the dendritic spike and the somatic action potential, we could also identify two distinct components in the slow ramp observed in the temporal derivative of somatic action potentials that followed a dendritic spike (Fig. 7F and H). The first component (red trace and shaded area) is a reflection of the steep depolarization that accompanies dendritic supra-linearities and is therefore present whenever a dendritic spike is initiated. When a somatic action potential is generated as a consequence of a dendritic spike, this first component underlies and is followed by a second one (shaded grey area), which ultimately leads to the steeper depolarization reflecting the invasion of the soma by the axonal action potential. We therefore conclude that the first component reflects the initiation of a dendritic spike, whereas the second one is a reflection of its successful forward propagation.

This is the first demonstration that the activation of distal excitatory inputs to entorhinal layer V neurons can initiate dendritic spikes, which can fully propagate to the soma to generate a somatic action potential. The initiation of active dendritic processes, such as dendritic spikes, could have fundamental consequences on the firing output (Gasparini & Magee, 2006) and therefore the functions of medial EC layer V neurons.

## Discussion

In this work, we have characterized the features of the synapses made by proximal and distal afferents onto layer V principal neurons of the medial EC of the rat. The main findings are: (1) EC layer V neurons receive excitatory glutamatergic synaptic contacts at distal dendritic locations; (2) distal synapses differ from proximal ones mainly in the amplitude of the putative unitary excitatory response; (3) entorhinal layer V neurons do not show the greater  $I_h$  density at distal dendritic locations that is observed in CA1 pyramidal neurons and layer V neocortical neurons; (4) the activation of distal inputs can initiate dendritic spikes that fully propagate to the soma. To our knowledge, this is the first characterization of functional excitatory inputs to the distal dendrites of entorhinal layer V neurons. This evidence and the ability of these inputs to engage the intrinsic membrane properties to initiate active dendritic events may alter the traditional view of the role of these neurons in memory processing and formation.

EC layer V neurons are the main recipient of the hippocampal output, which terminates in the deep layers, therefore targeting the basal and proximal portion of the apical dendrites of these neurons (Sørensen & Shipley, 1979). Most layer V neurons have long apical dendrites, which branch in complex tufts in the superficial layers (Hamam *et al.* 2000). Imaging techniques have demonstrated the presence of spines throughout the whole dendritic tree and their relatively high density at distal locations and tufts (Lingenhohl & Finch, 1991; Gasparini 2011). These spines could be contacted by fibres extending across the superficial layers and carrying sensory information, such as axons from the postrhinal and the piriform cortices (Burwell & Amaral, 1998a). Our data show that, indeed, distal excitatory synapses, characterized by significant slower rise time constants than proximal ones (as expected because of a more extensive dendritic filtering; Rall, 1967), can be activated by electrically stimulating the superficial layers of the EC or by placing a stimulating electrode at  $\sim 400 \mu\text{m}$  from the soma. While further investigations are needed to characterize the origin of these afferent fibres, our data suggest that EC layer V neurons might have access to information encoded by inputs to the superficial layers, challenging the traditional view that they only relay the processed hippocampal output back to various cortical areas.

In our initial experiments, we used GABA<sub>A</sub> receptor antagonists to isolate the excitatory responses; however, this pharmacological approach caused hyperexcitability in a significant fraction of the neurons examined (Fig. 2). To overcome this problem, we employed the  $\mu$ -opioid receptor agonist DAMGO, which was able to eliminate the inhibitory component of the EPSP–IPSP sequence without inducing the delayed burst firing observed in the presence of GABA<sub>A</sub> antagonists. An explanation for this outcome could be that, whereas GABA<sub>A</sub> antagonists completely abolished inhibitory transmission at the post-synaptic level, DAMGO reduces inhibitory transmission by reducing GABA release at the presynaptic level (Capogna *et al.* 1993; Svoboda & Lupica, 1998), therefore leaving inhibition sufficiently intact to prevent the hyperexcitability that is probably caused by recurrent excitatory activity. However, we cannot exclude possible differences in proximal *vs.* distal inhibitory tone that, due to the fact that DAMGO reduces and does not completely block inhibitory synaptic transmission, could potentially lead to recruitment of inhibitory synapses not affected by DAMGO during repetitive synaptic stimulation, therefore affecting some of our measurements.

We have found the amplitude of the putative unitary excitatory response to be  $\sim 1.5$  times larger for distal than for proximal synapses. This suggests the presence of mechanisms that counteract the electrotonic attenuation caused by the passive cable properties of dendrites (Rall, 1967) in EC layer V neurons. The nature

of such compensatory mechanisms could be either pre-synaptic or postsynaptic. Presynaptic mechanisms could include a larger size or higher number of released quanta (multivesicular release; see Lisman *et al.* 2007 for review), a higher number, higher density or different kinetics of Ca<sup>2+</sup> channels in the presynaptic terminal. On the other hand, likely postsynaptic compensatory mechanisms could encompass a higher dendritic input impedance at distal locations or different proportions of perforated *vs.* non-perforated glutamatergic synapses, as well as a distance-dependent scaling of the glutamatergic synaptic conductance, as has been shown to be the case for Schaffer collateral synapses in rat hippocampal CA1 pyramidal neurons (Magee & Cook, 2000; Andrásfalvy & Magee, 2001), and for other CNS preparations (Jansek & Redman, 1973; Alvarez *et al.* 1997). In particular, as in CA1 neurons, the synaptic scaling could be due to a higher postsynaptic AMPA receptor density (Smith *et al.* 2003), but it could also be the result of a higher conductance or open probability of individual AMPA receptor channels. The fact that PPF was not significantly different for proximal and distal inputs (see Fig. 3G) would favour the notion of postsynaptic compensatory mechanisms for entorhinal layer V neurons. Using a multicompartmental model we also found that the difference in amplitude in our experimental recordings could be accounted for by a synaptic conductance that was approximately three times as large at distal synapses than at the proximal ones; such an increase is comparable to what has been reported for CA1 pyramidal neurons (Magee & Cook, 2000).

Proximal and distal excitatory synaptic responses were mediated purely by glutamate; glutamatergic AMPA receptor antagonists blocked most of the excitatory component, and NMDA receptor antagonists always removed the remaining synaptic depolarization. On the other hand, as expected, the NMDA antagonist D,L-APV significantly decreased the amplitude and accelerated the decay of the responses, suggesting a significant role of NMDA-mediated synaptic transmission at both proximal and distal synaptic sites, and therefore the potential for a high level of plasticity at both sets of synapses (Collingridge *et al.* 2004).

One of the most significant results of our characterization of excitatory inputs is that h-channels appear to contribute to dendritic excitability in entorhinal layer V neurons far less than in hippocampal CA1 and neocortical layer V pyramidal neurons. Most of the neurons we recorded from did not show a prominent sag during 500 ms hyperpolarizing steps, as opposed to what has been reported for CA1 hippocampal and neocortical layer V neurons (Pape, 1996); in addition, the steady state input resistance under control conditions was much higher than for CA1 neurons (Magee, 1998). As a consequence, the blockade of  $I_h$  by ZD7288 had a

much smaller effect on the input resistance than what is observed in CA1 pyramidal neurons (Magee, 1999; and our Supplemental Material). Even more interesting, the effect of ZD7288 on temporal summation was location independent in entorhinal layer V neurons, i.e. the increase in temporal summation caused by the blockade of  $I_h$  was not significantly different for proximal and distal inputs. We found that this conclusion held true for 20 Hz trains of five as well as 10 EPSPs, therefore excluding the possibility that differences between proximal and distal effects of ZD7288 could become apparent with higher numbers of synaptic stimuli. This lack of location dependence is in clear contrast with what has been reported for CA1 hippocampal and layer V neocortical pyramidal neurons, where the effect of ZD7288 on temporal summation is much larger at distal than at proximal locations (Magee, 1999; Williams & Stuart, 2000; and our Supplemental Material). Altogether, these data argue against a higher expression of  $I_h$  in the distal apical dendrites of entorhinal layer V neurons. To date, this is the only difference in the intrinsic dendritic excitability that has been demonstrated between entorhinal layer V neurons and CA1 pyramidal neurons (Gasparini, 2011). Even at a lower expression level,  $I_h$  modulation by neurotransmitters could still have significant effects on neuronal excitability, as shown in the case of dopamine for layer V neurons in the lateral EC (Rosenkranz & Johnston, 2006).

Finally, we have found that EC layer V cells are more likely to generate a somatic output upon stimulation of their proximal rather than distal afferents. A somatic action potential was evoked by proximal stimulation in all the neurons tested, but only in about two-thirds of those where distal stimulation was employed even at the maximal intensity of stimulation (10 mA). In addition, a spike was generally obtained at a lower intensity of stimulation for proximal than for distal spikes. This result could be the consequence of a lower density of excitatory afferents to the distal dendrites compared with that of hippocampal/subicular fibres at proximal locations (Kloosterman *et al.* 2003), or of a less efficient transfer of information from distal synapses than from proximal ones due to the larger dendritic filtering. In this regard, it is interesting to notice that in more than a quarter of the neurons that were able to fire in response to distal stimulation the somatic action potential was the consequence of a spike generated in the dendrites that had fully propagated to the soma. This feature was revealed by the presence of a slow rising phase preceding the faster rising somatic action potential in the temporal derivative of the somatic voltage signal (Fig. 7F; Gasparini *et al.* 2004), and it was confirmed by the fact that the hyperpolarization of the somatic membrane potential could weaken forward propagation and uncouple the initiation of a dendritic spike from the generation of a somatic action potential. In these conditions, the somatic recordings

showed a spikelet, that is the reflection of a spike initiated in the dendrites that does not fully propagate to the soma (Golding *et al.* 2002; Gasparini *et al.* 2004). This is the first demonstration of the initiation of active dendritic processes in entorhinal layer V neurons. These distally initiated regenerative dendritic events would increase the efficacy of distal inputs at the soma, and potentially change the characteristics of the action potential output in the soma/axon region, as shown for CA1 pyramidal neurons (Gasparini & Magee, 2006). In addition, dendritic spikes could contribute to the postsynaptic depolarization and calcium entry that could lead to long-term potentiation of distal synapses (Golding *et al.* 2002). From the shape and duration of the action potentials recorded at the soma, as well as the spikelet observed at hyperpolarized potentials, we tend to conclude that these are fast  $\text{Na}^+$  dendritic spikes, similar to those observed in CA1 neurons (Golding *et al.* 2002; Gasparini *et al.* 2004), rather than  $\text{Ca}^{2+}$ /NMDA receptor-dependent spikes that are most often seen in neocortical layer V neurons (Schiller *et al.* 1997). This feature could be attributed to the fact that the EC layer V neurons show a gradient of A-type  $\text{K}^+$  channels along the apical dendrite similar to that found in CA1 pyramidal neurons (Gasparini, 2011), which in our experimental configuration would tend to limit the activation of dendritic  $\text{Ca}^{2+}$  channels. However, we cannot exclude that the coincident stimulation of proximal and distal afferent fibres could evoke dendritic plateau potentials in these neurons, such as those recorded in CA1 pyramidal neurons (Takahashi & Magee, 2009).

In summary, our results indicate that EC layer V principal neurons receive functional excitatory synaptic contacts at distal dendritic locations ( $\geq 400 \mu\text{m}$  from the soma), which would give them access to information encoded by inputs to the superficial layers in addition to the inputs from the hippocampus impinging on their proximal and basal dendrites. These distal inputs are bound to have fundamental implications for the integrative role of EC layer V cells in memory formation and consolidation.

## References

- Alvarez FJ, Dewey DE, Harrington DA & Fyffe RE (1997). Cell-type specific organization of glycine receptor clusters in the mammalian spinal cord. *J Comp Neurol* **379**, 150–170.
- Anderson P, Storm J & Wheal HV (1987). Thresholds of action potentials evoked by synapses on the dendrites of pyramidal cells in the rat hippocampus in vitro. *J Physiol* **383**, 509–526.
- Andrásfalvy BK & Magee JC (2001). Distance-dependent increase in AMPA receptor number in the dendrites of adult hippocampal CA1 pyramidal neurons. *J Neurosci* **21**, 9151–9159.
- Braak H & Braak E (1991). Neuropathological staging of Alzheimer-related changes. *Acta Neuropathol* **82**, 239–259.

- Burwell RD & Amaral DG (1998a). Cortical afferents of the perirhinal, postrhinal, and entorhinal cortices of the rat. *J Comp Neurol* **398**, 179–205.
- Burwell RD & Amaral DG (1998b). Perirhinal and postrhinal cortices of the rat: interconnectivity and connections with the entorhinal cortex. *J Comp Neurol* **391**, 293–321.
- Caballero-Bleda M & Witter MP (1993). Regional and laminar organization of projections from the presubiculum and parasubiculum to the entorhinal cortex: an anterograde tracing study in the rat. *J Comp Neurol* **328**, 115–129.
- Canto CB, Wouterlood FG & Witter MP (2008). What does the anatomical organization of the entorhinal cortex tell us? *Neural Plast* **2008**, 381243.
- Capogna M, Gähwiler BH & Thompson SM (1993). Mechanism of mu-opioid receptor-mediated presynaptic inhibition in the rat hippocampus in vitro. *J Physiol* **470**, 539–558.
- Colbert CM & Johnston D (1996). Axonal action-potential initiation and Na<sup>+</sup> channel densities in the soma and axon initial segment of subicular pyramidal neurons. *J Neurosci* **16**, 6676–6686.
- Collingridge GL, Isaac JT & Wang YT (2004). Receptor trafficking and synaptic plasticity. *Nature Rev Neurosci* **5**, 952–962.
- Eichenbaum H & Lipton PA (2008). Towards a functional organization of the medial temporal lobe memory system: role of the parahippocampal and medial entorhinal cortical areas. *Hippocampus* **18**, 1314–1324.
- Fyhn M, Molden S, Witter MP, Moser EI & Moser MB (2004). Spatial representation in the entorhinal cortex. *Science* **305**, 1258–1264.
- Gasparini S (2011). Distance- and activity-dependent modulation of spike back-propagation in layer V neurons of the medial entorhinal cortex. *J Neurophysiol* **105**, 1372–1379.
- Gasparini S & DiFrancesco D (1997). Action of the hyperpolarization-activated current (I<sub>h</sub>) ZD 7288 in hippocampal CA1 neurons. *Pflugers Arch* **435**, 99–106.
- Gasparini S & Magee JC (2006). State-dependent dendritic computation in hippocampal CA1 pyramidal neurons. *J Neurosci* **26**, 2088–2100.
- Gasparini S, Migliore M & Magee JC (2004). On the initiation and propagation of dendritic spikes in CA1 pyramidal neurons. *J Neurosci* **24**, 11046–11056.
- Golding NL, Staff NP & Spruston N (2002). Dendritic spikes as a mechanism for cooperative long-term potentiation. *Nature* **418**, 326–331.
- Hamam BN, Kennedy TE, Alonso A & Amaral DG (2000). Morphological and electrophysiological characteristics of layer V neurons of the rat medial entorhinal cortex. *J Comp Neurol* **418**, 457–472.
- Hanson JE, Emond MR & Madison DV (2006). Blocking polysynaptic inhibition via opioid receptor activation isolates excitatory synaptic currents without triggering epileptiform activity in organotypic hippocampal slices. *J Neurosci Methods* **150**, 8–15.
- Hargreaves EL, Rao G, Lee I & Knierim JJ (2005). Major dissociation between medial and lateral entorhinal input to dorsal hippocampus. *Science* **308**, 1792–1794.
- Hines ML & Carnevale NT (1997). The NEURON simulation environment. *Neural Comp* **9**, 1179–1209.
- Hyman BT, Van Hoesen GW, Damasio AR & Barnes CL (1984). Alzheimer's disease: cell-specific pathology isolates the hippocampal formation. *Science* **225**, 1168–1170.
- Insausti R, Herrero MT & Witter MP (1997). Entorhinal cortex of the rat: cytoarchitectonic subdivisions and the origin and distribution of cortical efferents. *Hippocampus* **7**, 146–183.
- Iansek R & Redman SJ (1973). The amplitude, time course and charge of unitary excitatory post-synaptic potentials evoked in spinal motoneurone dendrites. *J Physiol* **234**, 665–688.
- Jahr CE & Stevens CF (1990). A quantitative description of NMDA receptor-channel kinetic behavior. *J Neurosci* **10**, 1830–1837.
- Jones RS (1987). Complex synaptic responses of entorhinal cortical cells in the rat to subicular stimulation in vitro: demonstration of an NMDA receptor-mediated component. *Neurosci Lett* **81**, 209–214.
- Jones RS & Heinemann U (1988). Synaptic and intrinsic responses of medial entorhinal cortical cells in normal and magnesium-free medium in vitro. *J Neurophysiol* **59**, 1476–1496.
- Kloosterman F, Witter MP & Van Haeften T (2003). Topographical and laminar organization of subicular projections to the parahippocampal region of the rat. *J Comp Neurol* **455**, 156–171.
- Kohler C (1986). Intrinsic connections of the retrohippocampal region in the rat brain. II. The medial entorhinal area. *J Comp Neurol* **246**, 149–169.
- Lingenhohl K & Finch DM (1991). Morphological characterization of rat entorhinal neurons in vivo: soma-dendritic structure and axonal domains. *Exp Brain Res* **84**, 57–74.
- Lisman JE, Raghavachari S & Tsien RW (2007). The sequence of events that underlie quantal transmission at central glutamatergic synapses. *Nat Rev Neurosci* **8**, 597–609.
- Magee JC (1998). Dendritic hyperpolarization-activated currents modify the integrative properties of hippocampal CA1 pyramidal neurons. *J Neurosci* **18**, 7613–7624.
- Magee JC (1999). Dendritic I<sub>h</sub> normalizes temporal summation in hippocampal CA1 neurons. *Nat Neurosci* **2**, 508–514.
- Magee JC & Cook EP (2000). Somatic EPSP amplitude is independent of synapse location in hippocampal pyramidal neurons. *Nat Neurosci* **3**, 895–903.
- Makara JK, Losonczy A, Wen Q & Magee JC (2009). Experience-dependent compartmentalized dendritic plasticity in rat hippocampal CA1 pyramidal neurons. *Nat Neurosci* **12**, 1485–1477.
- Naber PA, Caballero-Bleda M, Jorritsma-Byham B & Witter MP (1997). Parallel input to the hippocampal memory system through peri- and postrhinal cortices. *Neuroreport* **8**, 2617–2621.
- Pape HC (1996). Queer current and pacemaker: the hyperpolarization-activated cation current in neurons. *Annu Rev Physiol* **58**, 299–327.
- Raastad M, Storm JF & Andersen P (1992). Putative single quantum and single fiber excitatory postsynaptic currents show similar amplitude range and variability in rat hippocampal slices. *Eur J Neurosci* **4**, 113–117.
- Rall W (1967). Distinguishing theoretical synaptic potentials computed for different soma-dendritic distributions of synaptic input. *J Neurophysiol* **30**, 1138–1168.

- Rosenkranz JA & Johnston D (2006). Dopaminergic regulation of neuronal excitability through modulation of  $I_h$  in layer V entorhinal cortex. *J Neurosci* **26**, 3229–3244.
- Sayer RJ, Friedlander MJ & Redman SJ (1990). The time course and amplitude of EPSPs evoked at synapses between pairs of CA3/CA1 neurons in the hippocampal slice. *J Neurosci* **10**, 826–836.
- Scharfman HE (2002). The parahippocampal region in temporal lobe epilepsy. In *The Parahippocampal Region: Organization and Role in Cognitive Function*, ed. Witter MP & Wouterlood FG, pp. 321–340. Oxford University Press, London.
- Schiller J, Schiller Y, Stuart G & Sakmann B (1997). Calcium action potentials restricted to distal apical dendrites of rat neocortical pyramidal neurons. *J Physiol* **505**, 605–616.
- Schwarcz R & Witter MP (2002). Memory impairment in temporal lobe epilepsy: the role of entorhinal lesions. *Epilepsy Res* **50**, 161–177.
- Smith MA, Ellis-Davies GC & Magee JC (2003). Mechanism of the distance-dependent scaling of Schaffer collateral synapses in rat CA1 pyramidal neurons. *J Physiol* **548**, 245–258.
- Sørensen KE & Shipley MT (1979). Projections from the subiculum to the deep layers of the ipsilateral presubicular and entorhinal cortices in the guinea pig. *J Comp Neurol* **188**, 313–333.
- Steward O & Scoville SA (1976). Cells of origin of entorhinal cortical afferents to the hippocampus and fascia dentate of the rat. *J Comp Neurol* **169**, 347–370.
- Svoboda KR & Lupica CR (1998). Opioid inhibition of hippocampal interneurons via modulation of potassium and hyperpolarization-activated cation ( $I_h$ ) currents. *J Neurosci* **18**, 7084–7098.
- Swanson LW & Cowan WM (1977). An autoradiographic study of the organization of the efferent connections of the hippocampal formation in the rat. *J Comp Neurol* **172**, 49–84.
- Swanson LW & Kohler C (1986). Anatomical evidence for direct projections from the entorhinal area to the entire cortical mantle in the rat. *J Neurosci* **6**, 3010–3023.
- Takahashi H & Magee JC (2009). Pathway interactions and synaptic plasticity in the dendritic tuft regions of CA1 pyramidal neurons. *Neuron* **62**, 102–111.
- Talbot K & Arnold SE (2002). The parahippocampal region in schizophrenia. In *The Parahippocampal Region: Organization and Role in Cognitive Function*, ed. Witter MP & Wouterlood FG, pp. 297–320. Oxford University Press, London.
- Tolner EA, Kloosterman F, van Vliet EA, Witter MP, Lopes da Silva FH & Gorter JA (2005). Presubiculum stimulation in vivo evokes distinct oscillations in superficial and deep entorhinal cortex layers in chronic epileptic rats. *J Neurosci* **25**, 8755–8765.
- Williams SR & Stuart GJ (2000). Site independence of EPSP time course is mediated by dendritic  $I_h$  in neocortical pyramidal neurons. *J Neurophysiol* **83**, 3177–3182.
- Witter MP & Amaral DG (1991). Entorhinal cortex of the monkey: V. Projections to the dentate gyrus, hippocampus, and subicular complex. *J Comp Neurol* **307**, 437–459.
- Witter MP & Wouterlood FG (2002). *The Parahippocampal Region. Organization and Role in Cognitive Function*. Oxford University Press, UK.
- Wouterlood FG, van Haften T, Eijkhoudt M, Baks-te-Bulte L, Goede PH & Witter MP (2004). Input from the presubiculum to dendrites of layer-V neurons of the medial entorhinal cortex of the rat. *Brain Res* **1013**, 1–12.

#### Author contributions

S.G. designed the study; V.M. and O.J. performed the experiments; V.M., O.J. and S.G. analysed the data; V.M., O.J. and S.G. wrote the paper and approved the final version of the manuscript.

#### Acknowledgements

This work was supported by the National Institutes of Health (R01 grants NS035865 and NS069714). We would like to acknowledge the contribution of Carmen Canavier and the LSUHSC Computational Core to the simulations using the NEURON multicompartmental model.